

Tideglusib Inhibits Pif1 Helicase of *Bacteroides* sp. via an Irreversible and Cys-380-Dependent Mechanism

Xianglian Zhou,* Yuting Pan, Yi Qu, and Xisong Ke*

Cite This: *ACS Omega* 2022, 7, 31289–31298

Read Online

ACCESS |



Metrics & More

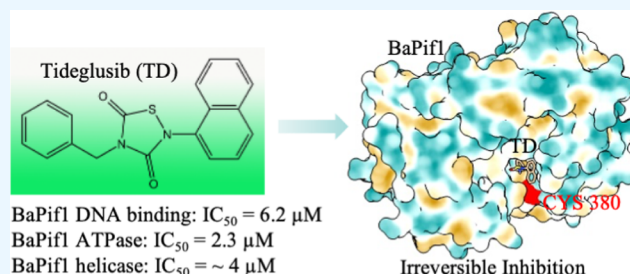


Article Recommendations



Supporting Information

ABSTRACT: Pif1 helicase plays multiple roles in maintaining genome stability, which is an attractive therapeutic target for helicase-related diseases, while small molecules targeting Pif1 are not yet available. In this study, we performed a fluorescence polarization-based high-throughput screening and identified that an FDA-approved drug, Tideglusib (TD), could inhibit the DNA-binding activity ($IC_{50} = 6.2 \pm 0.4 \mu\text{M}$) and ATPase and helicase activity ($IC_{50} = 2\text{--}4 \mu\text{M}$) of *Bacteroides* sp. Pif1 (BaPif1), which was also confirmed with human Pif1. In addition, the TD analogue TDZD-8 displayed similar inhibitory effects on Pif1 activities. Notably, TD irreversibly inhibited BaPif1 and severely induced BaPif1 aggregation. Furthermore, inhibition of BaPif1 by TD was significantly attenuated in the presence of dithiothreitol, indicating that TD could be a thiol-reactive compound. We also identified that Cys-380 of BaPif1 is critical for the inhibition by TD, suggesting that TD inhibits BaPif1 via an irreversible and Cys-380-dependent mechanism.



1. INTRODUCTION

Helicases are enzymes that couple the hydrolysis of ATP to the unwinding of double-stranded nucleic acids or translocating along with single-stranded nucleic acids. They are critical in many aspects of nucleic acid metabolism, including DNA repair, replication, recombination, and chromatin remodeling.^{1,2} The Pif1 helicase family is evolutionarily conserved from bacteria to humans and plays multiple roles in the maintenance of genomic homeostasis.^{3–5} Pif1 could inhibit telomere elongation and de novo telomere formation of both chromosomes and double-strand breaks (DSBs).^{6,7} It also functions in Okazaki fragment maturation,^{8–11} promoting fork progression at hard-to-replicate regions such as highly transcribed tRNA genes^{12–14} and G-quadruplex (G4) structures^{15–17} and stimulating repair-associated DNA synthesis with Pol δ during break-induced replication (BIR).^{18–20}

Recently, attention has been paid to the cellular functions of human Pif1 (hPif1). The depletion of hPif1 by siRNA resulted in a delayed S-phase, indicating a role in the completion of DNA replication.²¹ Additionally, several studies found that hPif1 physically interacts with the proliferating cell nuclear antigen (PCNA) to promote BIR which is a conserved homologous recombination (HR) pathway for DNA double-strand break repair (DSBR).^{18,22} Indeed, hPif1 is recruited to the site of DNA damage and facilitates DNA resection, specifically for the sequences prone to form G4 structures.²³ Also, the helicase activity of hPif1 is indispensable for BIR and the normal level of crossover HR.^{20,23} Furthermore, hPif1 has been proved to be required for the maintenance of replication fork progression during tumorigenesis, especially during

replication stress induced by genotoxic drugs or ionizing radiation, such as chemotherapy and radiotherapy.^{24,25} hPif1 has therefore been proposed as a cancer therapy target.^{26–28} However, no small-molecule inhibitors of Pif1 helicases have been reported before.

Extensive biochemical studies have revealed characteristics of Pif1 helicases, suggesting that the activities of Pif1 helicases are conserved from bacteria to humans.^{29–34} Like hPif1, the roles of Pif1 helicases in bacteria have been implicated in maintaining prokaryotic telomere, resolving DNA/RNA hybrid structures, and unwinding G4 DNA.³⁵ Intriguingly, Pif1 of *Bacteroides* sp. 3-1-23 (BsPif1) more resembles hPif1 than *Saccharomyces cerevisiae* Pif1 (ScPif1) in terms of substrate binding specificity, helicase activity, and mode of action.³¹ In addition, Pif1 of *Bacteroides* sp. 2-1-16 (BaPif1) is essentially the same helicase as BsPif1 except for a single amino acid substitution at position 138, and its crystal structure is similar to that of hPif1.²⁹

Tideglusib (TD), under the family of thiadiazolidinone, was first investigated for its role as a neuroprotective agent mediated by PPAR- γ activation, both in vitro and in vivo.³⁶ Functional studies revealed that TD was an ATP-non-

Received: June 7, 2022

Accepted: August 15, 2022

Published: August 25, 2022



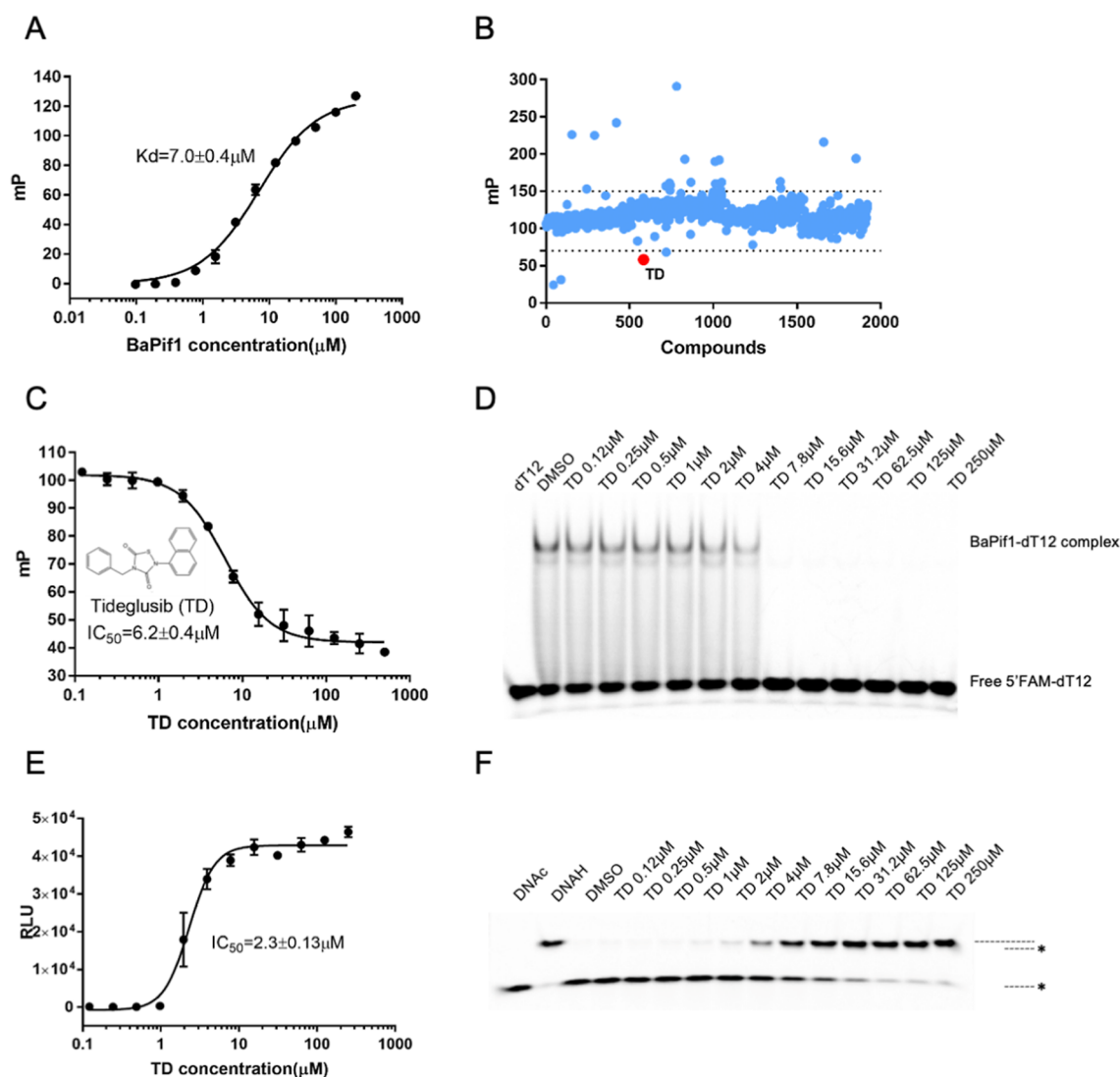


Figure 1. Identification of inhibitors of BaPif1 from an FP-based screening system. (A) Binding assays of different concentrations of BaPif1 protein and 1 μM FAM-labeled dT18 using the FP method. (B) FP-based HTS of the 1917 compounds. (C) FP-based IC_{50} assay of the effect of TD on the DNA-binding activity of BaPif1. (D) The disruption effect of TD on the interaction between BaPif1 and dT12 was examined by the F-EMSA assay. (E) IC_{50} assay of the inhibition effect of TD on the ATPase activity of BaPif1. (F) The inhibition effect of TD on the helicase activity of BaPif1 was detected by the helicase assay.

competitive inhibitor of GSK-3 β .³⁷ Further enzymological studies reported that TD inhibits GSK-3 β irreversibly, as demonstrated by the lack of recovery in enzyme function even after withdrawal of the unbound drug.³⁸ Although commonly, the irreversible inhibitors covalently bind to their target enzymes,³⁹ there is still no clear evidence that TD binds covalently to GSK-3 β .³⁸ Cys-199 in the GSK-3 β active site plays an important role in TD's activity, and the inhibitory potencies of TD are significantly attenuated by the presence of reducing agents.⁴⁰ However, the detailed mechanism of TD is complex and remains elusive.

2. RESULTS

2.1. TD Is an Inhibitor of BaPif1. Pif1 is a multifunctional helicase with no inhibitors being reported before. To identify novel small-molecule inhibitors of Pif1, we established an in vitro fluorescence polarization (FP)-based high-throughput screening (HTS) system for potential inhibitors of Pif1–DNA interaction. The affinity between purified Pif1 of *Bacteroides* sp.

2-1-16 (BaPif1) protein and the synthetic fluorescein amidite (FAM)-labeled oligo dT18 was confirmed via the FP assay. As shown in Figure 1A, the binding curve of different concentrations of the BaPif1 protein against 1 μM labeled dT18 was well displayed, and the K_d value was 7.0 μM . Finally, we used the 10 μM BaPif1 protein to do screening to produce enough FP values. With the established HTS system, primary screening was performed for an FDA-approved drug library containing 1917 compounds, among which TD was a positive hit (Figure 1B). The FP assay showed that the IC_{50} value of TD was $6.2 \pm 0.4 \mu\text{M}$ (Figure 1C). This inhibitory effect was also supported by the fluorescent electrophoretic mobility shift assay (F-EMSA) results (Figure 1D), which indicate that TD could block the binding of single-stranded DNA (ssDNA) to the BaPif1 protein. To address whether TD also inhibits the ATP hydrolysis activity and the unwinding activity of BaPif1, we further conducted assays to determine the ATPase and helicase activity in the presence of different TD concentrations. ATP hydrolysis was inhibited with the increasing TD

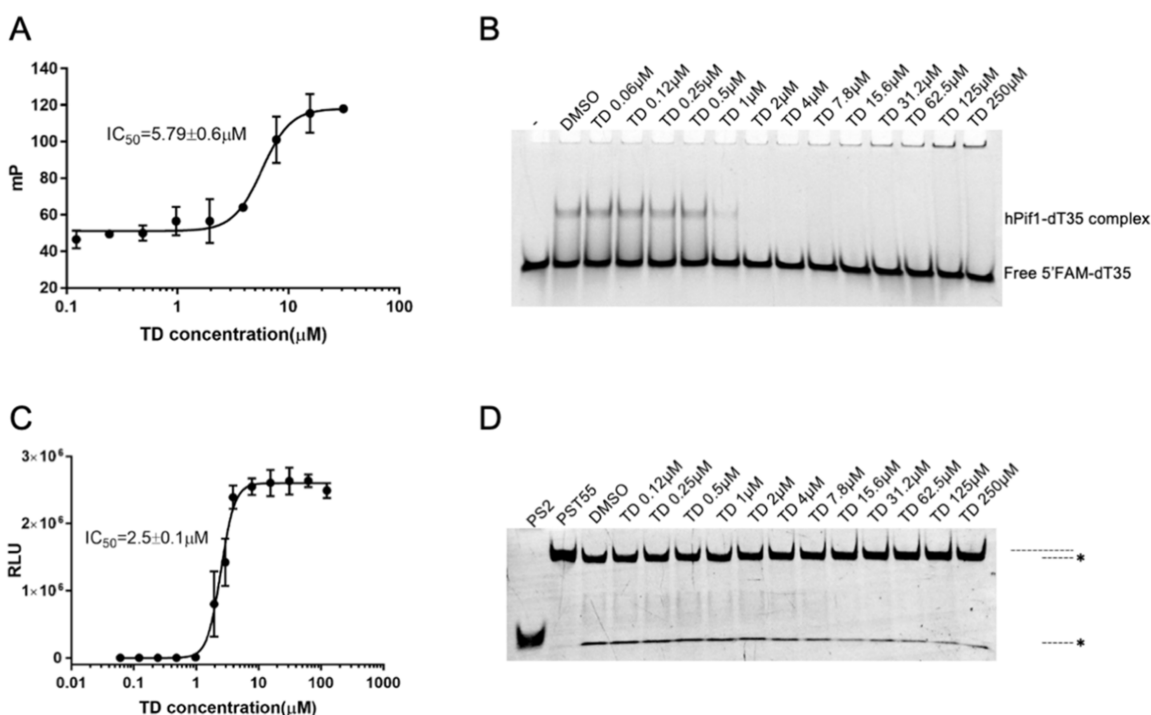


Figure 2. TD acts as an inhibitor of hPif1 proteins. (A) FP-based IC_{50} assay of the effect of TD on the DNA-binding activity of hPif1-HD. (B) The disruption effect of TD on the interaction between hPif1-HD and dT35 was examined by the F-EMSA assay. (C) IC_{50} assay of the inhibition effect of TD on the ATPase activity of hPif1-HD. (D) The inhibition effect of TD on the helicase activity of hPif1-HD was detected by the helicase assay.

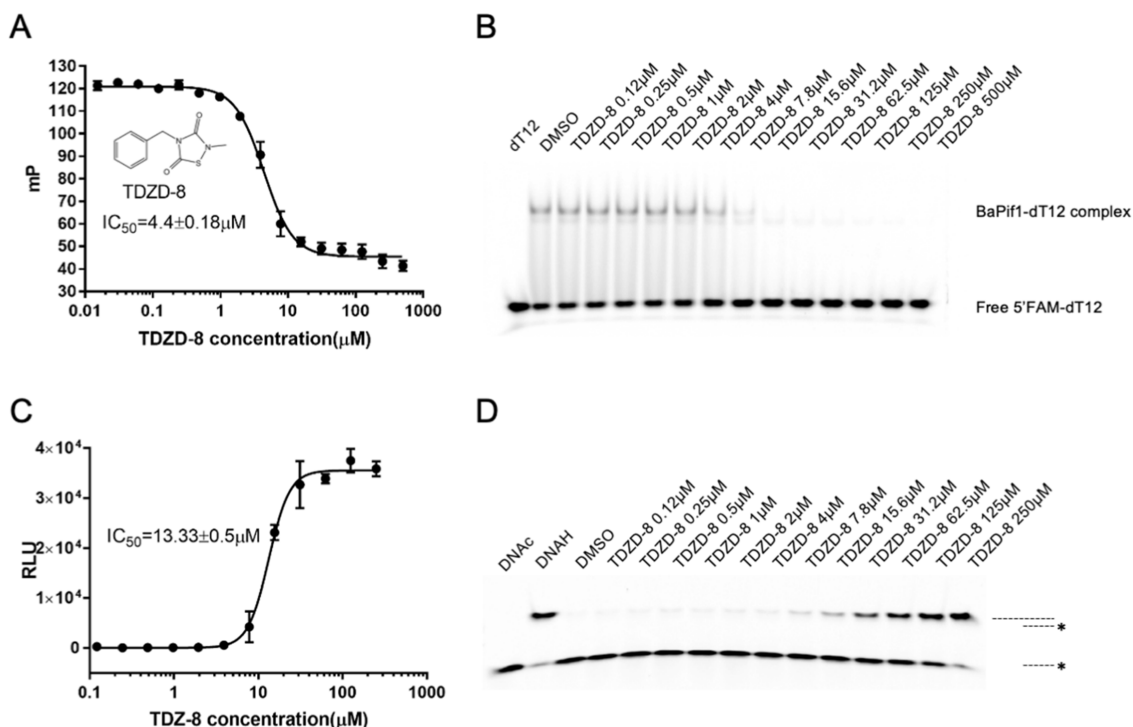


Figure 3. TDZD-8, a TD analogue, inhibits the activity of Bapif1. (A) FP-based IC_{50} assay of the effect of TDZD-8 on the DNA-binding activity of Bapif1. (B) The disruption effect of TDZD-8 on the interaction between Bapif1 and dT12 was examined by the F-EMSA assay. (C) IC_{50} assay of the inhibition effect of TDZD-8 on the ATPase activity of Bapif1. (D) The inhibition effect of TDZD-8 on the helicase activity of Bapif1 was detected by the helicase assay.

concentration, and the IC_{50} value was $2.3 \pm 0.13 \mu$ M (Figure 1E). The unwinding activity of Bapif1 was notably inhibited at 4μ M (Figure 1F). These data highlighted that TD was an inhibitor of Bapif1.

2.2. TD Is an Inhibitor of the hPif1 Protein. Pif1 is conserved from prokaryotes to eukaryotes.^{3–5} To address whether TD also functions as an inhibitor of hPif1, we further expressed and purified the helicase domain (HD) of hPif1.

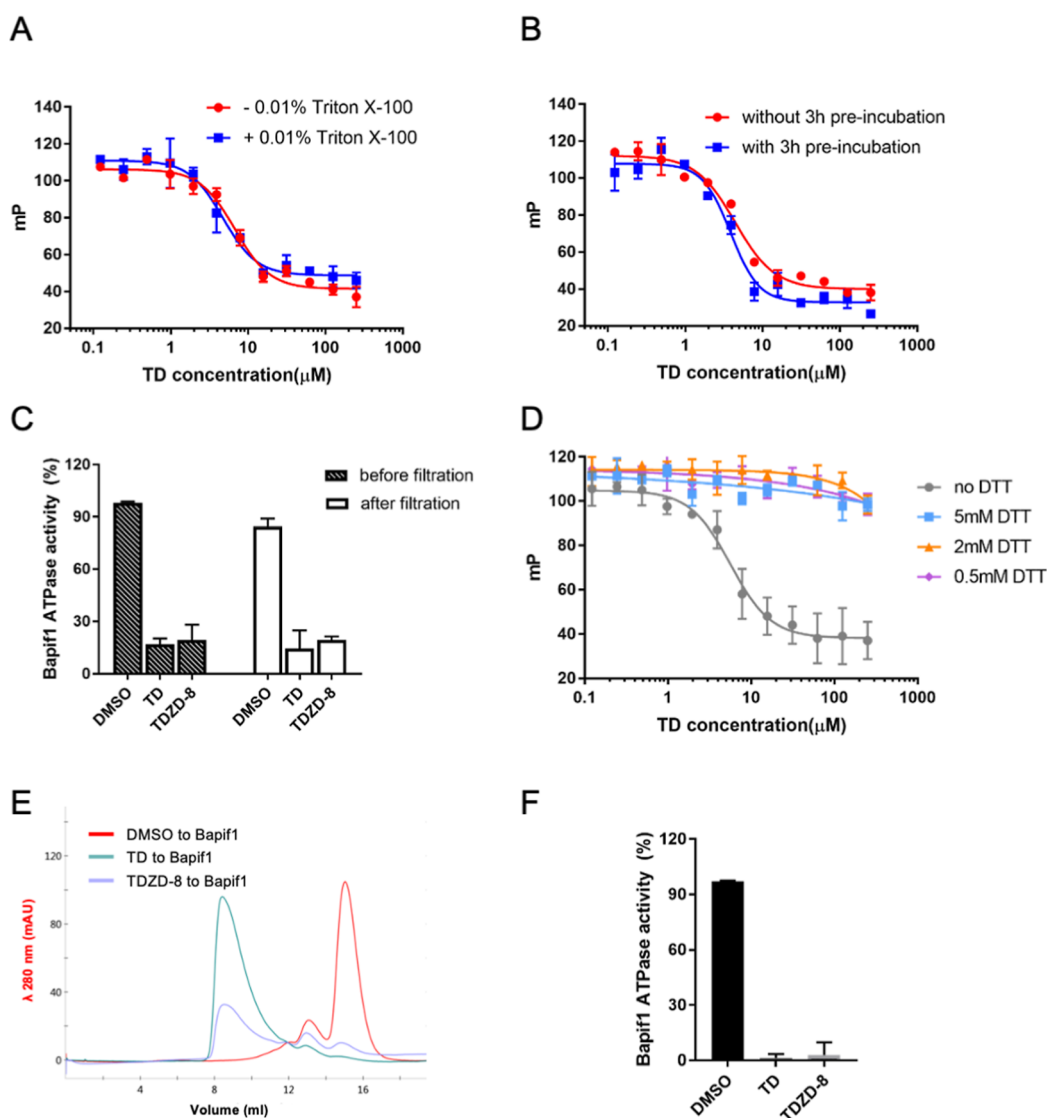


Figure 4. TD irreversibly inhibits Bapif1. (A) Effect of 0.01% v/v freshly prepared Triton X-100 on TD's inhibition of Bapif1 in the FP-based assay. (B) Dose–response curves for inhibition of Bapif1 with and without 3 h pre-incubation with TD were examined by an FP-based assay. (C) Percent inhibition of Bapif1 ATPase activity for TD and TDZD-8 after the filtration–dilution experiment. (D) The effect of the reducing agent DTT on the DNA-binding inhibition by TD of Bapif1 was detected by an FP-based assay. (E) TD- and TDZD-8-induced Bapif1 aggregation analyzed by size exclusion chromatography. (F) ATPase activity of Bapif1 at the peak collected by size exclusion chromatography in (E).

Unlike Bapif1, hPif1-HD did not bind oligonucleotides of 25 bases or less, as previously reported.^{41,42} Thus, FAM-labeled dT35 was used to detect the DNA-binding activity of hPif1-HD. We first confirmed the inhibition effect of TD on hPif1-HD's DNA-binding activity via the FP assay. The IC₅₀ value for TD to disrupt the interaction between hPif1-HD and DNA is $5.79 \pm 0.6 \mu\text{M}$ (Figure 2A). The F-EMSA assay confirmed that TD could markedly inhibit the DNA-binding activity of hPif1-HD at $2 \mu\text{M}$ as well (Figure 2B). In addition, TD also significantly inhibited the ATPase activity of hPif1-HD, and the IC₅₀ value was $2.5 \pm 0.1 \mu\text{M}$ (Figure 2C). Compared with Bapif1, the helicase activity of hPif1-HD was very low, which is consistent with previous reports.^{41,42} Also, more protein and a lengthier 5' overhang of the substrates were needed to initiate the unwinding reaction of hPif1-HD. Thus, a substrate with a 20 bp dsDNA portion and 5' oligo dT55 tail and $20 \mu\text{M}$ optimized hPif1-HD protein were used for helicase detection. In the titration experiment, helicase activity was inhibited with

TD at $7.8 \mu\text{M}$ (Figure 2D). These results suggested that TD also functions as an inhibitor of hPif1.

2.3. TD Analogue TDZD-8 Inhibits the Activity of Bapif1. To identify TD analogues that might be better inhibitors of Bapif1, another analogue TDZD-8 was purchased and tested. Compared with TD, TDZD-8 has a smaller molecular weight and better water solubility. TDZD-8 displayed a similar inhibitory effect to TD on the DNA-binding activity of Bapif1, with an IC₅₀ value of $4.4 \pm 0.18 \mu\text{M}$ (Figure 3A). The inhibition was also verified by F-EMSA results (Figure 3B), which suggested that TDZD-8 could block the binding of ssDNA to Bapif1 at $7.8 \mu\text{M}$. However, TDZD-8 was a less efficient inhibitor than TD in terms of ATPase activity as the IC₅₀ value was $13.33 \pm 0.5 \mu\text{M}$ which increased sixfold than that of TD (Figure 3C). Additionally, TDZD-8 inhibited the unwinding activity of Bapif1 at $15.6 \mu\text{M}$, which was 4 times that of TD (Figure 3D). Therefore, TDZD-8 also inhibits the activity of Bapif1, although its inhibition of ATPase

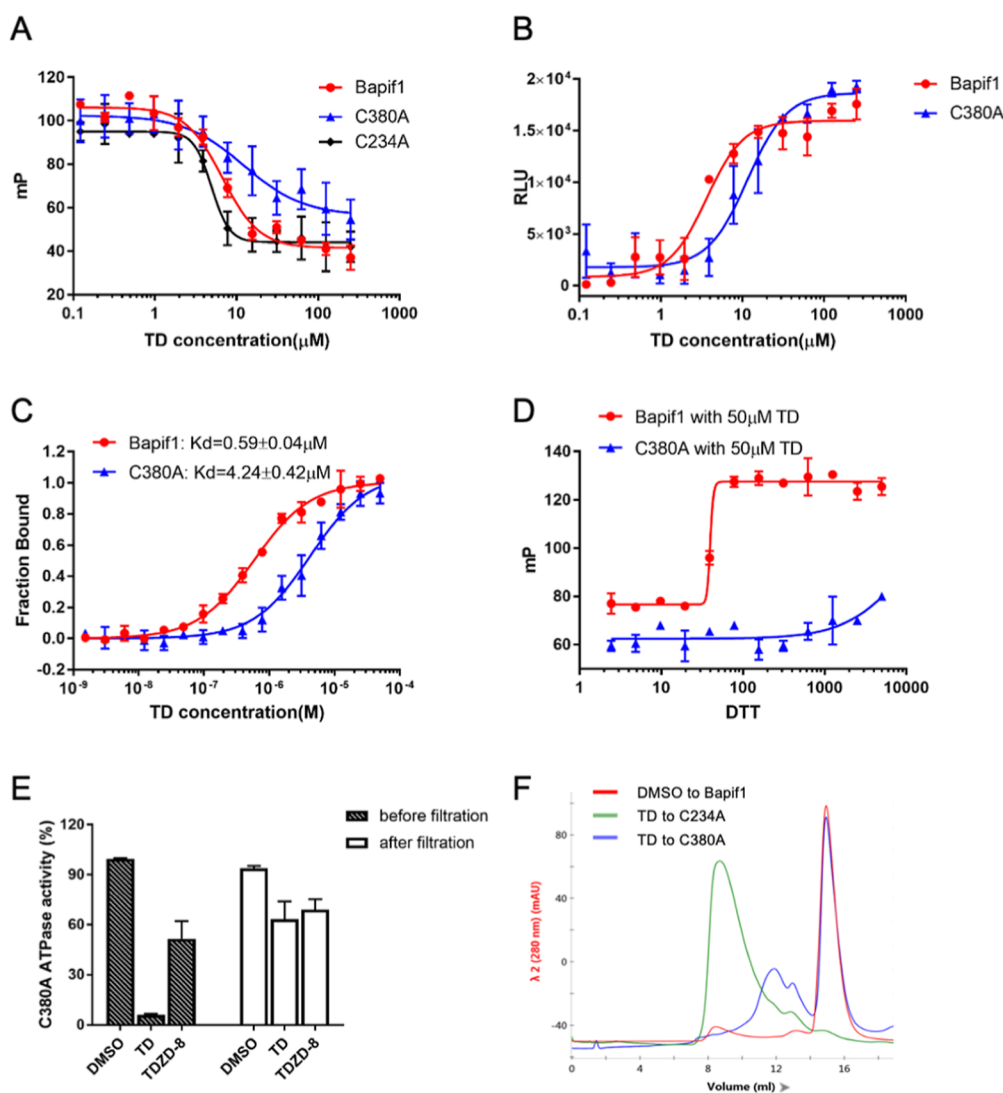


Figure 5. Effects of BaPif1 Cys-380 on TD inhibition. (A) Effects of Cys-234 and Cys-380 mutations on TD inhibition of BaPif DNA-binding activity. (B) Effects of Cys-380 mutation on TD inhibition of BaPif1 ATPase activity. (C) The binding affinity of TD to the wild-type BaPif1 or C380A mutant was examined by the MST assay. (D) Dose–response curves of DTT on the DNA-binding inhibition by $50 \mu\text{M}$ TD of the BaPif1 or C380A mutant detected by the FP-based assay. (E) Percent inhibition of C380A mutant ATPase activity for TD and TDZD-8 after the filtration–dilution experiment. (F) TD-induced C234A mutant aggregation while having no effect on the C380A mutant analyzed by size exclusion chromatography.

and helicase activities is not as efficient as that of TD. Additionally, TDZD-8 also functions as an inhibitor of hPif1 (Figure S1).

2.4. TD Irreversibly Inhibits BaPif1. To investigate whether TD is pan-assay interference compounds (PAINS)⁴³ for BaPif1, we detected the inhibitory activities of TD and TDZD-8 in the presence of 0.01% v/v freshly prepared Triton X-100 buffer in the FP assay. The results showed that the small amounts of the nonionic detergent did not affect the inhibitory activities of TD or TDZD-8 (Figures 4A and S2A). Previous work has demonstrated that TD was an irreversible inhibitor of GSK-3 β .³⁸ More generally, a time-dependent increase in apparent inhibitory potency suggests irreversible binding.³⁹ To illustrate whether TD is also an irreversible inhibitor of Pif1, we investigated the dose–response of TD and TDZD-8 with and without preincubation. As shown in Figures 4B and S2B, preincubation slightly increased the potency of TD and TDZD-8. To further confirm this, we decided to test the

reversibility of the inhibition by running filtration experiments. As observed in Figure 4C, the inhibition caused by $50 \mu\text{M}$ TD or TDZD-8 remained after the free, unbound drug had been removed by three consecutive filtration and dilution cycles, causing a 1000-fold dilution of the drugs. Accordingly, it is reasonable to expect that the inhibition effect caused by TD or TDZD-8 on BaPif1 was irreversible. As demonstrated by the previous study,⁴⁰ the inhibition potency of TD on GSK-3 β was significantly diminished in the presence of the reducing agents. Thus, we also explored the effect of dithiothreitol (DTT) on TD's ability to inhibit BaPif1. As shown in Figure 4D, the inhibition was significantly overcome in the buffer containing 0.5 mM DTT, suggesting that the mechanism of reactivity could be through sulfhydryl modification, a mechanism in common with the previous study of TD's inhibition on GSK-3 β .^{38,40} Additionally, we also observed that $30 \mu\text{M}$ BaPif1 incubated with $100 \mu\text{M}$ TD for 30 min could strongly induce the aggregation of BaPif1 analyzed by size exclusion

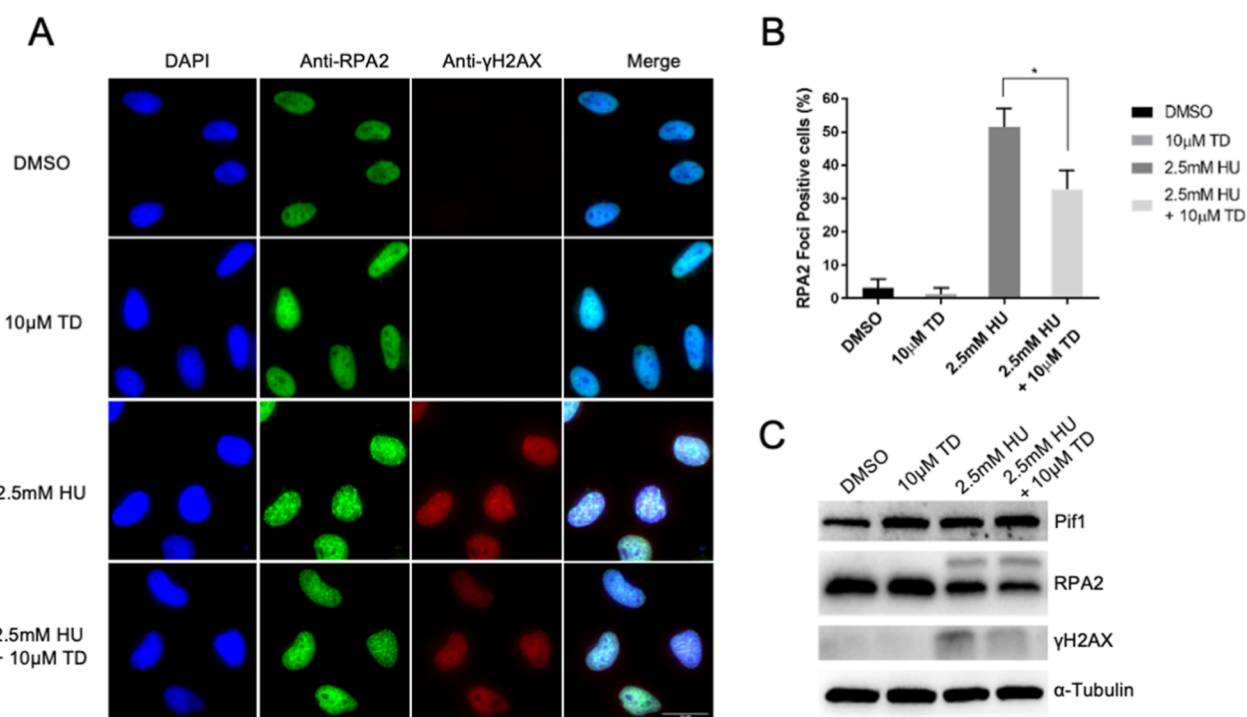


Figure 6. TD inhibits RPA foci formation in HeLa cells. (A) Representative images of RPA2 and γ H2AX staining after treatment with the indicated compounds. (B) Quantification of the percentage of RPA-foci-positive cells shown in (A). (C) Western blot of HeLa cell lysates with antibodies against Pif1, RPA2, and γ H2AX after treatment with the indicated compounds.

chromatography which might explain the irreversible inhibition pattern shown by TD and other structurally related compounds, such as TDZD-8 (Figure 4E,F).

2.5. Cys-380 Is Critical for the Inhibition by TD of BaPif1. To identify the potential cysteines involved in TD inhibition, we performed the sequence alignment and compared the structures of hPif1-HD and BaPif1 (Figure S2F).²⁹ Then, we selected two cysteine residues Cys-234 and Cys-380 of BaPif1 for further study. Each cysteine was mutated to alanine, and the activity of TD on the mutants was analyzed via the FP assay. As shown in Figure 5A, the C380A mutant was less sensitive to this compound compared with the wild-type, while the C234A mutant showed little change. It was noticeable that TD still had significant inhibition effect on the C380A mutant, suggesting that the Cys-380 residue is involved but not essential for the inhibitory activity of the compound. This also was confirmed by the ATPase assay (Figure 5B) and microscale thermophoresis (MST) binding assay (Figure 5C) using C380A's ATPase activity with TD. The IC_{50} value of TD on C380A's ATPase activity increased 3.2-fold against the wild-type (Figure 5B). Also, the K_d value of TD to C380A increased 7.2-fold compared with that of the wild-type. Given that the possible interaction with Cys-380 might involve the formation of a disulfide bond with the sulfur atom of the TD ring, the effect of the reducing agent (DTT) on the C380A mutant was also explored. As shown in Figures 5D and S3D, a low concentration of DTT could significantly abolish the DNA-binding inhibition of 50 μ M TD on BaPif1 (IC_{50} = 39.91 mM), while DTT almost showed no effect on the C380A mutant (>240-fold). Interestingly, the inhibition effect of TD on C380A's ATPase activity was reversible as detected by filtration experiments (Figure 5E). This observation was also confirmed by size exclusion chromatography that the 30 μ M C380A mutant protein incubated with 100 μ M TD for 30 min

could not induce the aggregation of C380A which was very different from wild-type BaPif1 (Figure 5F). Consequently, these results indicated that the mechanism of the inhibition of BaPif1 by TD involves Cys-380. However, the detailed mechanism needs further investigation.

2.6. TD Inhibits Replication Protein A Foci Formation in HeLa Cells. Pif1 is involved in multiple DNA transactions, including regulation of telomere stability, replication induced by DSBs, maturation of Okazaki fragments, and G4s resolution.^{3–5} A previous study has determined that Pif1 depletion results in reduced DNA damage sensitivity and HR efficiency which led to deflection in the replication protein A (RPA) foci formation in the Pif1-deficient cells.²³ More importantly, the helicase activity of Pif1 was essential for this phenotype.²³ To further confirm that TD acts as an inhibitor of Pif1 in cells, we detected whether TD could also inhibit RPA foci formation. As shown in Figure 6A,B, treatment of HeLa cells with 2.5 mM hydroxyurea (HU) could efficiently induce RPA foci formation, while 10 μ M TD combined with 2.5 mM HU could significantly reduce 20% of the RPA foci formation which was consistent with the observation in cells transfected with an siRNA against Pif1.²³ To validate this observation, we also detected the protein level of Pif1, RPA, and γ H2AX by western blot. As shown in Figure 6C, the protein level of both Pif1 and RPA did not alter, and the DNA damage response protein γ H2AX was slightly decreased in 10 μ M TD combined with 2.5 mM HU treatment. Thus, our data collectively suggested that TD inhibits RPA foci formation and slightly affects the DNA damage response.

3. DISCUSSION

In this study, we demonstrated that TD is a potent inhibitor of Pif1 utilizing molecular assays. We also investigated the mechanism of inhibition. According to the FP assay, TD

could inhibit the DNA-binding activity of BaPif1 with an IC_{50} value of $6.2 \pm 0.4 \mu\text{M}$ (Figure 1C). Also, biochemical assays demonstrated that TD also inhibited the ATPase and helicase activity of BaPif1 with IC_{50} values of 2–4 μM (Figure 1E,F). The inhibitory effect of TD on hPif1 was similar to that of BaPif1 in terms of DNA-binding activity and ATPase and helicase activity (Figure 2). Furthermore, TD had an inhibitory effect on hPif1 in living cells (Figure 6).

Moreover, our data demonstrated that TD is an irreversible inhibitor of Pif1 (Figure 4). This was evidenced by the lack of recovery of ATPase activity once the unbound drug was removed by the filtration experiments (Figure 4C). This is consistent with the previous finding that TD inhibits GSK-3 β irreversibly.³⁸ As Cys-199 in the GSK-3 β active site plays an important role in TD's activity and the inhibitory potencies of TD are significantly attenuated by the presence of reducing agents,⁴⁰ we speculated that TD inhibits Pif1 in a similar manner. This was confirmed by FP experiments with DTT (Figure 4D) and cysteine residue mutation assays (Figure 5). To test whether TD covalently modifies Pif1, we also performed high-performance liquid chromatography–mass spectrometry (HPLC–MS) on BaPif1 samples treated with TD (Figure S2C–E). HPLC–MS has not revealed any difference between the BaPif1-TD sample and BaPif1 alone, illustrating that either there is no covalent modification or it is too subtle to be detected by the methodologies used. Also, this fact might be consistent with the previous studies that TD covalently binds to Cys-199 of GSK-3 β , but none of the currently available experimental evidence supports this possibility unequivocally.³⁸

Mutating Cys-380 of BaPif1 to an alanine displayed reduced sensitivity to TD, indicating that Cys-380 is involved in the mechanism of inhibition. It is noticeable that the mutation of Cys-380 into alanine did not affect the DNA-binding and ATPase activities of BaPif1 (Figure S3B,C). Additionally, a low concentration of DTT could significantly induce the reversibility of the DNA-binding inhibition of BaPif1 by 50 μM TD ($IC_{50} = 39.91 \text{ mM}$), while the TD inhibition of the C380A mutant had little effect (>240-fold) (Figure S5D). Interestingly, the inhibition of C380A's ATPase activity by TD was reversible as detected by filtration experiments (Figure S5E). This observation was also confirmed by size exclusion chromatography that the 30 μM C380A mutant protein incubated with 100 μM TD for 30 min could not induce the aggregation of C380A which was very different from wild-type BaPif1 (Figure S5F). Altogether, these results demonstrate that interaction between Cys-380 and TD is involved in the mechanism of inhibition.

Previous studies have evaluated the activity of TD in a panel of kinases, including as many as 68 kinases.³⁸ The fact that only 10 of the 26 “Cys-conserved” kinases were significantly inhibited by 10 μM TD suggests that specific interactions should be involved. However, the selectivity of TD for other helicases should be further investigated. Nevertheless, the nonspecific effects of TD and its analogues should not be ignored, and concerns about the thiazolidinone functional groups' potential non-specific or covalent mode of action may hinder the development of these molecules toward therapeutic potential candidates.⁴⁴ The development of cysteine-reactive small-molecule inhibitors into useful research probes and therapeutic agents is challenging yet surmountable. Indeed, covalent drugs have proved to be successful therapies for various indications, and successes in the clinic, mainly in the

field of kinase inhibitors, are existing proof that safe covalent inhibitors can be designed and employed to develop effective treatments.^{45,46} Here, we found that TD inhibits BaPif1 via an irreversible and Cys-380-dependent mechanism, and these findings may guide the development of novel isoform-specific inhibitors.

4. MATERIALS AND METHODS

4.1. Protein Purification. The gene encoding Pif1 of *Bacteroides* sp. 2-1-16 was synthesized and cloned into pGEX-6P-1 such that the expressed protein would have an N-terminal glutathione S-transferase (GST)-tagged protein. The construct was transformed into the expression host *E. coli* BL21 (DE3), and cells were grown in a lysogeny broth medium containing 100 mg/mL ampicillin at 37 °C until the OD_{600} reached 0.4–0.6. The cells were then induced by adding 0.1 mM isopropylthiogalactoside and grown at 18 °C for another 16 h. Cells were harvested by centrifugation. The cell pellet was resuspended in a buffer containing 20 mM Tris (pH 7.5), 500 mM NaCl, and 2 mM DTT and lysed by sonication. After centrifugation, the clarified cell lysate was incubated with glutathione sepharose 4B beads, and GST-tagged BaPif1 was eluted with the buffer consisting of buffer A and 25 mM reduced glutathione. The GST tag was cleaved by prescission protease, and the released BaPif1 was further purified to homogeneity by successive chromatographic steps involving glutathione sepharose 4B beads, anion ion exchange, and gel-filtration columns. Pure protein fractions in buffer containing 20 mM Tris (pH 7.5), 150 mM NaCl, and 2 mM DTT were used for the crystal screening. The selenomethionine-substituted single-site mutants of BaPif1, C234A, and C380A were also constructed in the same vector using two primers, with required mutation using polymerase chain reaction. All the mutants were purified with the same protocol as that of the wild-type BaPif1. The gene encoding the hPif1 (Q9H611) HD (aa200–641) was synthesized (GenScript, China) and cloned into pET-28a, such that the expressed proteins would have an N-terminal 6 \times His-tag. The plasmid was expressed in the *E. coli* BL21(DE3) strain, which was purified as recommended before by Co-NTA beads and then size exclusion chromatography (Superdex 200 increase 10/300 GL). Finally, all the proteins were concentrated in 20 mM Tris (pH 7.5), 150 mM NaCl and stored at –80 °C.

4.2. FP Assay. 5'FAM-labeled oligo dT18 was synthesized by Sangon (Shanghai, China). The HTS system based on BaPif1 and dT18 interaction was established with the FP technique. For the primary screening, the reaction includes 0.5 mg/mL BaPif1, 1 μM FAM-labeled dT18, and 100 μM compound in buffer A (25 mM Tris-HCl, pH 7.5, and 5 mM MgCl_2). A library including 1917 FDA-approved compounds (L1021, APEX-BIO) was screened. The reactions were incubated at room temperature for 10 min and then detected with a spark instrument (TECAN) at an excitation wavelength of 480 nm and an emission wavelength of 520 nm. TD was selected from the screening for further study. Dose-dependent assays of TD were carried out using the FP method with 0.5 μM FAM-labeled DNA substrates, 10 μM BaPif1 or 10 μM hPif1 (200–641), and different concentrations of TD in Tris buffer. All the assay was carried out without 2 mM DTT if there was no special mention. The IC_{50} value was determined by fitting the binding curves using GraphPad Prism 7.0.

4.3. F-EMSA Assay. Small molecules that inhibit the DNA-binding activity of BaPif1 or other proteins were examined

with fluorescent EMSA (F-EMSA). Oligonucleotides dT12 and dT35 were synthesized with a 5'-FAM label. The reactions were carried out with the addition of 50 nM oligonucleotides, 0.1 mg/mL BaPif1, or other proteins in buffer A and titrated with a varying concentration ligand to the final 10 μ L reaction mixture and incubated at 25 $^{\circ}$ C for 30 min. Then, samples were electrophoresed at 80 V for 50 min in 8% tris-borate-EDTA (TBE) gel, and the gel was imaged with ChemiDoc (Bio-Rad).

4.4. Helicase Activity. The helicase assay was done as recommended before.²⁹ Briefly, the oligos 5'-FAM-GCGCGGCCCGG-3' (DNAC) and 5'-TTTTTTTCCGGGGCCGCGC-3' (dH) were annealed to form the FAM-labeled duplex DNAH that was used as the substrate for the helicase reaction for BaPif1.²⁹ To detect hPif1(200-641) helicase activity, 5'-(T)55-CGAATTC-GAGCTCGGTACCC (PS1) and 5'-FAM-GTACC-GAGCTCGAATTCG (PS2) were annealed to form the FAM-labeled duplex PST55.⁴² For BaPif1, the reaction mixture was used containing 20 mM Tris-HCl (pH 7.5), 150 mM NaCl, 5 mM MgCl₂, 5% glycerol, 0.1 mg/mL BaPif1 helicase, 0.2 μ M DNAH, and 100 μ M trapper single-strand DNA (the same sequence to DNAC) and titrated with a varying concentration ligand. The reaction was initiated by adding 50 mM ATP and incubated at 37 $^{\circ}$ C for 10 min, and it was stopped by adding 0.5 mM ethylenediaminetetraacetic acid (EDTA). An aliquot of the reaction mixture was analyzed for strand unwinding by using 12% polyacrylamide gel electrophoresis in 0.5 \times TBE buffer. For hPif1(200-641), the reaction system was similar to that of BaPif1 except including 1 mg/mL hPif1(200-641) helicase, 20 nM PST55, and a different concentration ligand in Tris buffer. The reaction was initiated by adding 50 mM ATP and incubated at 37 $^{\circ}$ C for 30 min, and it was stopped by adding 0.5 mM EDTA. Then, samples were electrophoresed in 8% TBE gel. After electrophoresis, the gel was visualized using ChemiDoc (Bio-Rad).

4.5. ATPase Activity. Typically, the reaction consisted of 0.1 mg/mL BaPif1 or other proteins mixed with a series of diluted compounds as indicated in assay buffer (20 mM Tris-HCl, 150 mM NaCl, 5 mM MgCl₂, pH 7.5) in a final dimethyl sulfoxide (DMSO) concentration of 5% in a total volume of 20 μ L. The mixtures were incubated for 30 min at 25 $^{\circ}$ C; then, 100 nM ssDNA dH and 100 nM ATP were added to initiate the ATP hydrolase reaction. After incubation at 25 $^{\circ}$ C for 10 min, the reaction was stopped by adding 1 N NaOH, and the hydrolyzation of ATP in the reaction system was detected using an ATP Assay Kit (S0026, Beyotime) following the manufacturer's instructions in 384 wells. In this assay, the ATP concentration in the reaction system is coupled to the firefly luciferase. Luminescence was read using spark (TECAN) with an integration time of 1 s per well. Also, the data were analyzed using GraphPad Prism 7.0.

4.6. MST Assay. The purified proteins BaPif1 and C380A were labeled using the RED-NHS kit under the manufacturer's protocol (MO-L011, NanoTemper Technologies), and the fluorescent signals of the proteins were suitable for the detection using the Monolith NT.115 instrument (NanoTemper Technologies). For binding affinity detection, a 10 μ L protein sample was mixed with a 10 μ L ligand at various concentrations as indicated. Then, the mixture solutions were loaded into NT.115 standard coated capillaries or premium coated capillaries (NanoTemper Technologies), and the MST measurements were performed at 25 $^{\circ}$ C. The fluorescence

signal during the thermophoresis was monitored, and the change in fluorescence was analyzed using software. The K_d was calculated by fitting a standard binding curve to the series of diluted ligands. Also, data were analyzed using GraphPad Prism 7.0.

4.7. Filtration Experiments. The reversibility of BaPif1 inhibition was tested by filtration through Amicon Ultra-0.5 centrifugal filter devices (Millipore) with a cut-off of 10 kDa followed by dilution of the concentrated retentate. Samples of 0.1 mg/mL BaPif1 in the assay buffer described above were incubated with 5% DMSO or with a 50 μ M concentration of the tested compounds in 5% DMSO for 30 min and then filtered by centrifugation according to the manufacturer's instructions. The retentate sample was diluted 10-fold with assay buffer to recover the original volume. This procedure was repeated three times (total dilution was 1000-fold), and finally, the diluted retentate was used to measure the BaPif1 ATPase activity as described above.

4.8. Analytical Size Exclusion Chromatography. 400 μ L of 1.5 mg/mL BaPif1 or mutants containing 5% DMSO or containing 100 μ M TD was loaded onto a Superdex 200 Increase 10/300 GL column (GE) connected to an NGC chromatography system (Bio-Rad) and equilibrated with buffer A (20 mM Tris-HCl, pH 7.5, 150 mM NaCl, and 5 mM MgCl₂). Elution profiles were monitored by absorbance at 280 nm at 4 $^{\circ}$ C, and 0.5 mL fractions were collected and analyzed by the ATPase assay.

4.9. Immunofluorescence. For RPA foci visualization, HeLa cells were seeded in 48-well plates (Costar) for 24 h. After this, cells were treated with indicated ligands for 24 h. Then, cells were washed twice with phosphate buffered saline (PBS) followed by treatment with 4% paraformaldehyde (w/v) in PBS for 20 min to fix the cells. Following two washes with PBS, cells were permeabilized in 0.3% Triton X-100 and blocked with 5% bovine serum albumin in PBS. Then, cells were incubated with primary antibodies against RPA2 (ab2175, Abcam) and γ H2AX (2577S, CST) in a blocking solution overnight at 4 $^{\circ}$ C. The cells were washed again with PBS and then co-immunostained with the appropriate secondary fluorescent antibodies in blocking buffer. Cells were mounted with 0.1 mg/mL 4,6-diamidino-2-phenylindole (Beyotime) for nuclear staining. Images were captured with an ImageXpress Micro 4 microscope (Molecular Devices) using standard settings.

4.10. Western Blot. Cells were lysed using radio-immunoprecipitation assay (CST) containing a protease inhibitor (Thermo Fisher Scientific) at 4 $^{\circ}$ C. Proteins were quantified using the BCA protein quantification kit (Thermo Fisher Scientific). Also, proteins (10–30 μ g per lane) were separated by sodium dodecyl sulfate-polyacrylamide gel electrophoresis and then transferred onto polyvinylidene fluoride membranes (Millipore). Following this, the membranes were blocked with 5% non-fat milk for an hour. Later on, the membranes were incubated with primary antibodies anti-Pif1 (48377, Santa Cruz), anti-RPA2 (ab2175, Abcam), anti- γ H2AX (2577S, CST), and anti-GAPDH (5174, CST) overnight at 4 $^{\circ}$ C. After this, the membranes were incubated with HRP goat anti-mouse secondary antibodies (1:5000, CST) for 1 h, and an enhanced chemiluminescence detection reagent (NCM Biotech) was used to visualize the signal strength of the bands.

■ ASSOCIATED CONTENT

SI Supporting Information

The Supporting Information is available free of charge at <https://pubs.acs.org/doi/10.1021/acsomega.2c03546>.

TDZD-8 inhibition of the DNA-binding and ATPase and helicase activities of hPif1; HPLC–MS analysis of the effect of TD on BaPif1 and structural alignment of BaPif1 and hPif1-HD; and DNA-binding and ATPase activities of the C380A mutant (PDF)

■ AUTHOR INFORMATION

Corresponding Authors

Xianglian Zhou – Shanghai Frontiers Science Center of TCM Chemical Biology, Institute of Interdisciplinary Integrative Medicine Research, Shanghai University of Traditional Chinese Medicine, Shanghai 201203, China; orcid.org/0000-0001-8557-8853; Email: zhouxianglian@shutcm.edu.cn

Xisong Ke – Shanghai Frontiers Science Center of TCM Chemical Biology, Institute of Interdisciplinary Integrative Medicine Research, Shanghai University of Traditional Chinese Medicine, Shanghai 201203, China; orcid.org/0000-0001-7328-7354; Email: xisongke@shutcm.edu.cn

Authors

Yuting Pan – Shanghai Frontiers Science Center of TCM Chemical Biology, Institute of Interdisciplinary Integrative Medicine Research, Shanghai University of Traditional Chinese Medicine, Shanghai 201203, China

Yi Qu – Shanghai Frontiers Science Center of TCM Chemical Biology, Institute of Interdisciplinary Integrative Medicine Research, Shanghai University of Traditional Chinese Medicine, Shanghai 201203, China

Complete contact information is available at:

<https://pubs.acs.org/doi/10.1021/acsomega.2c03546>

Author Contributions

X.Z. conceived and designed the experiments; X.Z. and Y.P. performed the experiments; X.Z. and Y.Q. analyzed the data; X.Z. wrote the original draft; X.Z. and X.K. reviewed and edited the manuscript.

Funding

This work was supported by the Natural Science Foundation of China (31800668, 81703757, 81874210, and 81874319), the Science and Technology Commission of Shanghai Municipality (18401933500 and 21S11900900), the Shanghai Municipal Education Commission (2019-01-07-00-10-E00072 and 2021-01-07-00-10-E00116), the Shanghai Youth Talent Support Program, the Shuguang Project (19SG40), and the Program for Professor of Special Appointment (Eastern Scholar).

Notes

The authors declare no competing financial interest. The UniProt accession ID for human Pif1: Q9H611. The GenBank ID of the NCBI for *Bacteroides* sp. 2-1-16 Pif1: EEZ27408.1.

■ ABBREVIATIONS

TD, Tideglusib; FP, fluorescence polarization; HTS, high-throughput screening; RPA, replication protein A; EMSA, electrophoretic mobility shift assay

■ REFERENCES

- (1) Singleton, M. R.; Dillingham, M. S.; Wigley, D. B. Structure and mechanism of helicases and nucleic acid translocases. *Annu. Rev. Biochem.* **2007**, *76*, 23–50.
- (2) Lohman, T. M.; Tomko, E. J.; Wu, C. G. Non-hexameric DNA helicases and translocases: mechanisms and regulation. *Nat. Rev. Mol. Cell Biol.* **2008**, *9*, 391–401.
- (3) Bochman, M. L.; Sabouri, N.; Zakian, V. A. Unwinding the functions of the Pif1 family helicases. *DNA Repair* **2010**, *9*, 237–249.
- (4) Boulé, J. B.; Zakian, V. A. Roles of Pif1-like helicases in the maintenance of genomic stability. *Nucleic Acids Res.* **2006**, *34*, 4147–4153.
- (5) Byrd, A. K.; Raney, K. D. Structure and function of Pif1 helicase. *Biochem. Soc. Trans.* **2017**, *45*, 1159–1171.
- (6) Zhou, J. Q.; Monson, E. K.; Teng, S.-C.; Schulz, V. P.; Zakian, V. A. Pif1p Helicase, a Catalytic Inhibitor of Telomerase in Yeast. *Science* **2000**, *289*, 771–774.
- (7) Boulé, J.-B.; Vega, L. R.; Zakian, V. A. The yeast Pif1p helicase removes telomerase from telomeric DNA. *Nature* **2005**, *438*, 57–61.
- (8) Pike, J. E.; Henry, R. A.; Burgers, P. M. J.; Campbell, J. L.; Bambara, R. A. An alternative pathway for Okazaki fragment processing resolution of fold-back flaps by Pif1 helicase. *J. Biol. Chem.* **2010**, *285*, 41712–41723.
- (9) Pike, J. E.; Burgers, P. M. J.; Campbell, J. L.; Bambara, R. A. Pif1 helicase lengthens some Okazaki fragment flaps necessitating Dna2 nuclease/helicase action in the two-nuclease processing pathway. *J. Biol. Chem.* **2009**, *284*, 25170–25180.
- (10) Rossi, M. L.; Pike, J. E.; Wang, W.; Burgers, P. M. J.; Campbell, J. L.; Bambara, R. A. Pif1 helicase directs eukaryotic Okazaki fragments toward the two-nuclease cleavage pathway for primer removal. *J. Biol. Chem.* **2008**, *283*, 27483–27493.
- (11) Budd, M. E.; Reis, C. C.; Smith, S.; Myung, K.; Campbell, J. L. Evidence Suggesting that Pif1 Helicase Functions in DNA Replication with the Dna2 Helicase/Nuclease and DNA Polymerase δ . *Mol. Cell Biol.* **2006**, *26*, 2490–2500.
- (12) Tran, P. L. T.; Pohl, T. J.; Chen, C. F.; Chan, A.; Pott, S.; Zakian, V. A. PIF1 family DNA helicases suppress R-loop mediated genome instability at tRNA genes. *Nat. Commun.* **2017**, *8*, 15025.
- (13) Osmundson, J. S.; Kumar, J.; Yeung, R.; Smith, D. J. Pif1-family helicases cooperatively suppress widespread replication-fork arrest at tRNA genes. *Nat. Struct. Biol.* **2017**, *24*, 162–170.
- (14) Schauer, G. D.; Spenkelink, L. M.; Lewis, J. S.; Yurieva, O.; Mueller, S. H.; van Oijen, A. M.; O'Donnell, M. E. Replisome bypass of a protein-based R-loop block by Pif1. *Proc. Natl. Acad. Sci. U.S.A.* **2020**, *117*, 30354–30361.
- (15) Paeschke, K.; Bochman, M. L.; Garcia, P.; Cejka, P.; Friedman, K. L.; Kowalczykowski, S. C.; Zakian, V. A. Pif1 family helicases suppress genome instability at G-quadruplex motifs. *Nature* **2013**, *497*, 458–462.
- (16) Paeschke, K.; Capra, J. A.; Zakian, V. A. DNA Replication through G-Quadruplex Motifs Is Promoted by the *Saccharomyces cerevisiae* Pif1 DNA Helicase. *Cell* **2011**, *145*, 678–691.
- (17) Lopes, J.; Piazza, A. L.; Bermejo, R.; Kriegsman, B.; Colosio, A.; Teulade-Fichou, M. P.; Foiani, M.; Nicolas, A. G-quadruplex-induced instability during leading-strand replication. *EMBO J.* **2011**, *30*, 4033–4046.
- (18) Wilson, M. A.; Kwon, Y.; Xu, Y.; Chung, W. H.; Chi, P.; Niu, H.; Mayle, R.; Chen, X.; Malkova, A.; Sung, P.; et al. Pif1 helicase and Pol δ promote recombination-coupled DNA synthesis via bubble migration. *Nature* **2013**, *502*, 393–396.
- (19) Saini, N.; Ramakrishnan, S.; Elango, R.; Ayyar, S.; Zhang, Y.; Deem, A.; Ira, G.; Haber, J. E.; Lobachev, K. S.; Malkova, A. Migrating bubble during break-induced replication drives conservative DNA synthesis. *Nature* **2013**, *502*, 389–392.
- (20) Li, S.; Wang, H.; Jehi, S.; Li, J.; Liu, S.; Wang, Z.; Truong, L.; Chiba, T.; Wang, Z.; Wu, X. PIF1 helicase promotes break-induced replication in mammalian cells. *EMBO J.* **2021**, *40*, No. e104509.

- (21) Futami, K.; Shimamoto, A.; Furuichi, Y. Mitochondrial and nuclear localization of human Pif1 helicase. *Biol. Pharm. Bull.* **2007**, *30*, 1685–1692.
- (22) Buzovetsky, O.; Kwon, Y.; Pham, N. T.; Kim, C.; Ira, G.; Sung, P.; Xiong, Y. Role of the Pif1-PCNA Complex in Pol δ -Dependent Strand Displacement DNA Synthesis and Break-Induced Replication. *Cell Rep.* **2017**, *21*, 1707–1714.
- (23) Jimeno, S.; Camarillo, R.; Mejías-Navarro, F.; Fernández-Ávila, M. J.; Soria-Bretones, I.; Prados-Carvajal, R.; Huertas, P. The Helicase PIF1 Facilitates Resection over Sequences Prone to Forming G4 Structures. *Cell Rep.* **2018**, *25*, 3543.
- (24) Gagou, M. E.; Ganesh, A.; Phear, G.; Robinson, D.; Petermann, E.; Cox, A.; Meuth, M. Human PIF1 helicase supports DNA replication and cell growth under oncogenic-stress. *Oncotarget* **2014**, *5*, 11381–11398.
- (25) Gagou, M. E.; Ganesh, A.; Thompson, R.; Phear, G.; Sanders, C.; Meuth, M. Suppression of apoptosis by PIF1 helicase in human tumor cells. *Cancer Res.* **2011**, *71*, 4998–5008.
- (26) Yin, X.; Kan, D.; Ruan, J.; Wang, D.; Chai, Y.; Huang, S.; Zhang, B.; Wang, J.; Ji, X. Identifying PIF1 as a Potential Target of Wenzia Changfu Formula in Promoting Lung Cancer Cell Apoptosis: Bioinformatics Analysis and Biological Evidence. *Evid. base Compl. Alternative Med.* **2021**, *2021*, 9942462.
- (27) Wang, J.; Zhu, X.; Ying, P.; Zhu, Y. PIF1 Affects the Proliferation and Apoptosis of Cervical Cancer Cells by Influencing TERT. *Cancer Manage. Res.* **2020**, *12*, 7827–7835.
- (28) Chen, B.; Hua, Z.; Gong, B.; Tan, X.; Zhang, S.; Li, Q.; Chen, Y.; Zhang, J.; Li, Z. Downregulation of PIF1, a potential new target of MYCN, induces apoptosis and inhibits cell migration in neuroblastoma cells. *Life Sci.* **2020**, *256*, 117820.
- (29) Zhou, X.; Ren, W.; Bharath, S. R.; Tang, X.; He, Y.; Chen, C.; Liu, Z.; Li, D.; Song, H. Structural and Functional Insights into the Unwinding Mechanism of Bacteroides sp Pif1. *Cell Rep.* **2016**, *14*, 2030–2039.
- (30) Chen, W. F.; Dai, Y. X.; Duan, X. L.; Liu, N. N.; Shi, W.; Li, N.; Li, M.; Dou, S. X.; Dong, Y. H.; Rety, S.; et al. Crystal structures of the BsPif1 helicase reveal that a major movement of the 2B SH3 domain is required for DNA unwinding. *Nucleic Acids Res.* **2016**, *44*, 2949–2961.
- (31) Liu, N. N.; Duan, X. L.; Ai, X.; Yang, Y. T.; Li, M.; Dou, S. X.; Rety, S.; Deprez, E.; Xi, X. G. The Bacteroides sp. 3_1_23Pif1 protein is a multifunctional helicase. *Nucleic Acids Res.* **2015**, *43*, 8942–8954.
- (32) Dehghani-Tafti, S.; Levdikov, V.; Antson, A. A.; Bax, B.; Sanders, C. M. Structural and functional analysis of the nucleotide and DNA binding activities of the human PIF1 helicase. *Nucleic Acids Res.* **2019**, *47*, 3208–3222.
- (33) Lu, K. Y.; Chen, W. F.; Rety, S.; Liu, N. N.; Wu, W. Q.; Dai, Y. X.; Li, D.; Ma, H. Y.; Dou, S. X.; Xi, X. G. Insights into the structural and mechanistic basis of multifunctional *S. cerevisiae* Pif1p helicase. *Nucleic Acids Res.* **2017**, *46*, 1486–1500.
- (34) Su, N.; Byrd, A. K.; Bharath, S. R.; Yang, O.; Jia, Y.; Tang, X.; Ha, T.; Raney, K. D.; Song, H. Structural basis for DNA unwinding at forked dsDNA by two coordinating Pif1 helicases. *Nat. Commun.* **2019**, *10*, 5375.
- (35) Bochman, M. L.; Judge, C. P.; Zakian, V. A. The Pif1 family in prokaryotes: what are our helicases doing in your bacteria? *Mol. Biol. Cell* **2011**, *22*, 1955–1959.
- (36) Luna-Medina, R.; Cortes-Canteli, M.; Sanchez-Galiano, S.; Morales-Garcia, J. A.; Martinez, A.; Santos, A.; Perez-Castillo, A. NP031112, a thiadiazolidinone compound, prevents inflammation and neurodegeneration under excitotoxic conditions: potential therapeutic role in brain disorders. *J. Neurosci.* **2007**, *27*, 5766–5776.
- (37) Martinez, A.; Alonso, M.; Castro, A.; Dorronsoro, I.; Gelpi, J. L.; Luque, F. J.; Pérez, C.; Moreno, F. J. SAR and 3D-QSAR studies on thiadiazolidinone derivatives: exploration of structural requirements for glycogen synthase kinase 3 inhibitors. *J. Med. Chem.* **2005**, *48*, 7103–7112.
- (38) Domínguez, J. M.; Fuertes, A.; Orozco, L.; del Monte-Millán, M.; Delgado, E.; Medina, M. Evidence for Irreversible Inhibition of Glycogen Synthase Kinase-3 β by Tideglusib. *J. Biol. Chem.* **2012**, *287*, 893–904.
- (39) Aldrich, C.; Bertozzi, C.; Georg, G. I.; Kiessling, L.; Lindsley, C.; Liotta, D.; Merz, K. M., Jr.; Schepartz, A.; Wang, S. The Ecstasy and Agony of Assay Interference Compounds. *J. Med. Chem.* **2017**, *60*, 2165–2168.
- (40) Ghazanfari, D.; Noori, M. S.; Bergmeier, S. C.; Hines, J. V.; McCall, K. D.; Goetz, D. J. A novel GSK-3 inhibitor binds to GSK-3 β via a reversible, time and Cys-199-dependent mechanism. *Bioorg. Med. Chem.* **2021**, *40*, 116179.
- (41) Gu, Y.; Masuda, Y.; Kamiya, K. Biochemical analysis of human PIF1 helicase and functions of its N-terminal domain. *Nucleic Acids Res.* **2008**, *36*, 6295–6308.
- (42) George, T.; Wen, Q.; Griffiths, R.; Ganesh, A.; Meuth, M.; Sanders, C. M. Human Pif1 helicase unwinds synthetic DNA structures resembling stalled DNA replication forks. *Nucleic Acids Res.* **2009**, *37*, 6491–6502.
- (43) Pouliot, M.; Jeanmart, S. Pan Assay Interference Compounds (PAINS) and Other Promiscuous Compounds in Antifungal Research. *J. Med. Chem.* **2016**, *59*, 497–503.
- (44) Mathuram, T. L.; Reece, L. M.; Cherian, K. M. GSK-3 Inhibitors: A Double-Edged Sword?—An Update on Tideglusib. *Drug Res.* **2018**, *68*, 436–443.
- (45) De Vita, E. 10 years into the resurgence of covalent drugs. *Future Med. Chem.* **2021**, *13*, 193–210.
- (46) Singh, J.; Petter, R. C.; Baillie, T. A.; Whitty, A. The resurgence of covalent drugs. *Nat. Rev. Drug Discovery* **2011**, *10*, 307–317.